

Singularity index of the core-level x-ray photoemission spectrum from surface atoms

Masahiko Kato

Surface and Interface Laboratory, RIKEN (The Institute of Physical and Chemical Research), Wako, Saitama 351, Japan

(Received 17 May 1988)

We calculate the singularity index of the x-ray photoemission spectrum that is excited from a core level near a simple metal surface. Although the surface singularity index is generally different from the bulk singularity index, the former index has almost the same value as the latter. Moreover, using the Thomas-Fermi dielectric screening of point-charge-like core potentials, we investigate qualitatively the singularity index for physisorbed atoms.

Previous core-level x-ray photoemission spectra¹ (XPS) from metals were insensitive to the surface. These experiments showed that the observed spectral line could be well fitted by the Doniach-Šunjić (DS) line-shape function.² The DS line-shape function is

$$A(\epsilon) = \frac{\Gamma(1-\alpha) \cos[\frac{1}{2}\pi\alpha + (1-\alpha)\arctan(\epsilon/\gamma)]}{(\epsilon^2 + \gamma^2)^{(1-\alpha)/2}}, \quad (1)$$

where $\Gamma(x)$ is the gamma function and ϵ is the energy measured from the edge of the unbroadened spectrum, and γ^{-1} is the core-hole lifetime. Equation (1) has an asymmetric shape depending on the value of the singularity index, α , which is one of the parameters characterizing electronic excitations near the Fermi surface. Since surface electronic properties are different from the bulk properties, there is no reason to expect that the DS line-shape function should describe the XPS from the surface region. Even if the DS line-shape function is applicable, it is not obvious that the singularity index for the surface region should have the same value as the bulk singularity index. However, recent core-level XPS experiments³ with high surface sensitivity show that the DS line-shape function with the same values of parameters γ and α can equally well fit both the bulk and the surface components within experimental error. Nozières and de Dominicis⁴ showed that

$$\alpha = 2 \sum_l (2l+1) \left(\frac{\delta_l}{\pi} \right)^2, \quad (2)$$

where δ_l is the phase shift of the l th partial wave at the Fermi level. α is closely related to the screening mechanism of the core potential. Because of the different screening mechanism, the singularity index of the surface system is different from the bulk singularity index.

The singularity index has been calculated by several authors,⁵⁻⁷ but these calculations have been done only for homogeneous media. Even for inhomogeneous systems, Eq. (2) probably still holds if we define the generalized phase shifts⁸ appropriately. However, it seems difficult to deal with this type of equation in a direct manner. Hence, we generalize Langreth's method⁹ to the surface system. Although Langreth's singularity index is a low-order calculation with respect to the screened potential,

this method can be easily applied to the inhomogeneous system, particularly to the planar surface system, and still contain the essence of the physics involved.

We treat the metal using the jellium model. Let $\delta n(\mathbf{r})$ and $V(\mathbf{r})$ denote the induced electron density and the Coulomb repulsive interaction potential, respectively. We consider the Hamiltonian

$$\begin{aligned} H = & Ec^\dagger c + \int d^3r \psi^\dagger(\mathbf{r}) \frac{-\hbar^2 \nabla^2}{2m} \psi(\mathbf{r}) \\ & + \int d^3r \int d^3r' V(\mathbf{r}-\mathbf{r}') \delta n(\mathbf{r}) \delta n(\mathbf{r}') \\ & + \int d^3r U(\mathbf{r}) \delta n(\mathbf{r}) cc^\dagger, \end{aligned} \quad (3)$$

where c^\dagger and c are the creation and destruction operators for a core electron, respectively, $\psi^\dagger(\mathbf{r})$ and $\psi(\mathbf{r})$ are creation and destruction field operators for conduction electrons, respectively, and E is the core-electron eigenenergy. The interaction potential between the core electron and the conduction electron (core potential), $U(\mathbf{r})$, is treated in the same manner as Ref. 6. In this treatment, $U(\mathbf{r})$ can be expressed by

$$U(\mathbf{r}) = -\frac{1}{(2\pi)^3} \int d^3k \rho_{R_h}(\mathbf{k}) \frac{4\pi e^2}{k^2} e^{-i\mathbf{k}\cdot\mathbf{r}},$$

where $\rho_{R_h}(\mathbf{k})$ is the Fourier transform of the difference in core-electron density associated with the change in potential seen by the conduction electron when the core-electron is removed, and R_h indicates the core-hole position.

In the first part of this report, we use the Ashcroft pseudopotential in order to describe the core potential. In this case, we have

$$\begin{aligned} \rho_{R_h}(\mathbf{k}) = & [(Z+1)\cos(kr_c^*) - Z\cos(kr_c)] e^{i\mathbf{k}\cdot\mathbf{R}_h} \\ = & \rho(\mathbf{k}) e^{i\mathbf{k}\cdot\mathbf{R}_h}, \end{aligned} \quad (4)$$

where r_c , r_c^* , and Z are defined in Ref. 6. We assume that these parameters are independent of the core-hole position, \mathbf{R}_h . In the other part, we employ the point-charge approximation. This approximation combined with the Thomas-Fermi-type dielectric screening is rather informative for obtaining physical trend of the singularity index. In this treatment, r_c , r_c^* , and Z are set to zero, i.e.,

$\rho(\mathbf{k})=1$.

Under the sudden approximation, it is sufficient to know the core-electron Green function, $G_c(t) = -i\langle Tc(t)c^\dagger(0) \rangle$, in order to study the intrinsic effect.¹⁰ In what follows, we assume the system at the absolute zero for simplicity. By means of the standard method,⁶ we obtain

$$G_c = i\Theta(-t)\exp\left[-\frac{i}{\hbar}Et\right] \times \exp\left[-\int_0^\infty \frac{d\omega}{\omega} \alpha(\mathbf{R}_h, \omega)(1+i\omega t - e^{i\omega t})\right],$$

where $\Theta(x)$ is the step function and

$$\alpha(\mathbf{R}_h, \omega) = \frac{1}{\pi\hbar\omega} \text{Im}[S(\mathbf{R}_h, \omega)]. \quad (5)$$

$\alpha(\mathbf{R}_h, \omega)$ is named the *dynamical* singularity index. The singularity index is defined by the static limit of $\alpha(\mathbf{R}_h, \omega)$. In Eq. (4), $S(\mathbf{R}_h, \omega)$ is given by

$$S(\mathbf{R}_h, \omega) = -\int d^3r \int d^3r' U(\mathbf{r})P(\mathbf{r}, \mathbf{r}', \omega)U(\mathbf{r}'), \quad (6)$$

where $P(\mathbf{r}, \mathbf{r}', \omega)$ is the electronic polarization. Hence, $S(\mathbf{R}_h, \omega)$ is the self-energy of the charge distribution given by the Fourier inverse transform of Eq. (4).

We deal with $S(\mathbf{R}_h, \omega)$ by the dielectric response theory, and we treat the surface system as a semi-infinite degenerate electron gas bounded by an infinite step barrier¹¹ at $z=0$ (infinite barrier model). Then, $S(\mathbf{R}_h, \omega)$ can be expressed in terms of the bulk dielectric function. This model well describes the actual surface system which has a large work function. However, we note that the infinite barrier model may be a poor approximation for high electron density metals (the electron density parameter, $r_s < 2$).¹¹

Because of the translational invariance along the surface, $S(\mathbf{R}_h, \omega)$ is a function of the core-hole distance from the infinite barrier. Let a metal occupy the half space $z > 0$, and let z_h denote the position of the core hole. We decompose the wave vector \mathbf{k} into $\mathbf{k}=(\kappa, q)$. When we employ the Ashcroft pseudopotentials, we consider only the region of $z_h > r_c, r_c^*$. Using the electro-dynamical image charge method,¹² we obtain

$$S(z_h, \omega) = \frac{1}{(2\pi)^2} \int_{-\infty}^{\infty} d^2\kappa \left[\int_{-\infty}^{\infty} dq \frac{1-\epsilon}{\epsilon} \frac{[2\rho(\mathbf{k})\cos qz_h - e^{-|\kappa|z_h}]^2}{\kappa^2 + q^2} - \left[\int_{-\infty}^{\infty} dq \frac{1-\epsilon}{\epsilon} \frac{2\rho(\mathbf{k})\cos qz_h - e^{-|\kappa|z_h}}{\kappa^2 + q^2} \right]^2 / \left[I + \frac{\pi}{|\kappa|} \right] \right], \quad (7)$$

where $\epsilon = \epsilon(\mathbf{k}, \omega)$ is the bulk dielectric function, and

$$I = \int_{-\infty}^{\infty} dq \frac{1}{\kappa^2 + q^2} \frac{1}{\epsilon}.$$

For explicit calculation, we use the dielectric function,

$$\epsilon(\mathbf{k}, \omega) = 1 + \frac{\epsilon_{\text{RPA}}(\mathbf{k}, \omega) - 1}{1 - f(\mathbf{k})[\epsilon_{\text{RPA}}(\mathbf{k}, \omega) - 1]}, \quad (8)$$

where ϵ_{RPA} is the random-phase approximation dielectric function and $f(\mathbf{k})$ is the local correlation function. For numerical simplicity, we use Hubbard's expression of $f(\mathbf{k})$.¹³

Equations (5)–(8) yield the singularity index. Figure 1 shows the z_h dependence of the singularity indices, $\alpha(z_h, \omega=0)$, of Li, Na, and Al. Here we used the same values of XPS parameters (r_c, r_c^*, Z, r_s) as used in Ref. 6. The bulk singularity index α_b is given by $\lim_{z_h \rightarrow \infty} \alpha(z_h, 0)$. The calculated values of α_b for Li, Na, and Al are 0.235, 0.207, and 0.109, respectively. As shown in Fig. 1, $\alpha(z_h, 0)$ is enhanced near the metal surface. This enhancement is attributed to that of the electron density near the surface. However, $\alpha(z_h, 0)$ shows no oscillation such as the Friedel oscillation. We note that the infinite barrier at $z=0$ is not the position of first-layer atoms but the surface of electron gas. Accord-

ing to Ref. 11, in which the electron density calculated by the infinite-barrier model is compared with that calculated by the local-density functional theory,¹⁴ we find that the first-layer atom is located at a distance of about $5a_0$ for Li, $6a_0$ for Na, and $4a_0$ for Al from the surface of electron gas, where a_0 is the Bohr radius. Therefore, the

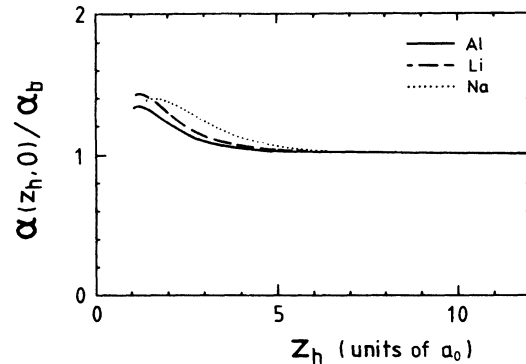


FIG. 1. The normalized singularity indices, $\alpha(z_h, 0)/\alpha_b$, as a function of the core-hole position, z_h . Each line is calculated with the same values of XPS parameters, r_c, r_c^*, Z , and r_s , as used in Ref. 6. The bulk singularity indices, α_b , of Li, Na, and Al are 0.235, 0.207, and 0.109, respectively. a_0 is the Bohr radius.

singularity index of the first layer atom is at most 5% larger than the bulk singularity index (see Fig. 1).

Figure 2 shows the dynamical singularity index of a Na atom which is located at $z_h = 5a_0$. Since $\alpha(z_h, \omega)$ is nearly constant up to the surface-plasmon frequency, $\omega_s = \omega_p / \sqrt{2}$, the DS line-shape function for simple metal surface atoms is fairly well defined.¹⁵

In the following, we employ the Thomas-Fermi-type dielectric screening of point-charge-like core potentials.

$$\alpha^{\text{TF}}(z_h, \omega) = \begin{cases} -\frac{e^2}{4\pi^3 \hbar} \frac{1}{\omega} \int_{-\infty}^{\infty} d^2 \kappa \text{Im} \left[\int_{-\infty}^{\infty} dq \frac{1-\epsilon}{\epsilon} \frac{(2 \cos q z_h - e^{-|\kappa| z_h})^2}{\kappa^2 + q^2} \right. \\ \left. - \left[\int_{-\infty}^{\infty} dq \frac{1-\epsilon}{\epsilon} \frac{2 \cos q z_h - e^{-|\kappa| z_h}}{\kappa^2 + q^2} \right]^2 / \left[I + \frac{\pi}{|\kappa|} \right] \right], & \text{for } z_h \geq 0, \\ -\frac{e^2}{2\pi^2 \hbar} \frac{1}{\omega} \int_{-\infty}^{\infty} \frac{d^2 \kappa}{|\kappa|} e^{2|\kappa| z_h} \text{Im} \left[\frac{|\kappa| I - \pi}{|\kappa| I + \pi} \right], & \text{for } z_h \leq 0. \end{cases} \quad (9)$$

Here ϵ represents the generalized Thomas-Fermi dielectric function

$$\epsilon_{\text{TF}} = 1 + \frac{k_{\text{TF}}^2}{k^2 [1 - i(\pi \omega / 2k v_F) \Theta(2k_F - k)]}, \quad (10)$$

where k_{TF} and k_F are the Thomas-Fermi and the Fermi wave numbers, respectively, and v_F is the Fermi velocity. Since Eq. (10) is appropriate only for small k and ω (see below), we will not discuss the dynamical singularity index but will study the static case only. For the bulk

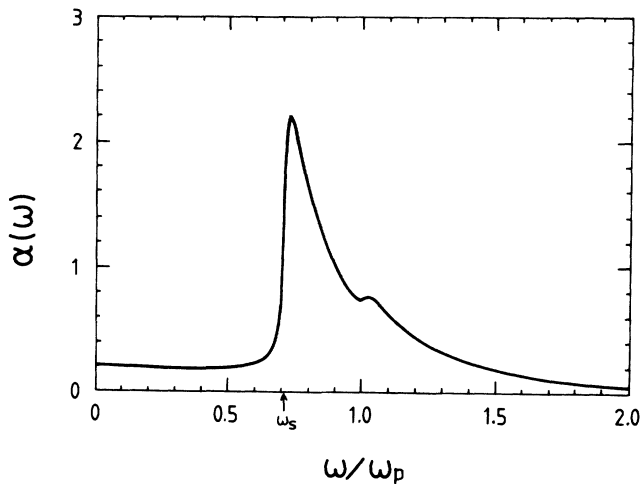


FIG. 2. The dynamical singularity index of a Na atom which is located at $z_h = 5a_0$. ω_p is the bulk-plasmon frequency. The surface-plasmon frequency, $\omega_s (= \omega_p / \sqrt{2})$, is indicated by the arrow. The main peak at ω_s is ascribed to the surface-plasmon excitation, and the shoulder at ω_p corresponds to the plasmon excitation. Taking account of a finite lifetime of plasmon, the curve is smoothed with a Gaussian, and full width at half maximum is 0.1 eV.

This treatment is simple and, moreover, useful in studying the z_h dependence of the singularity index. However, we note that the point-charge approximation becomes a good approximation in the case when a characteristic screening length is large compared with the core-hole size. In the point-charge limit, the singularity index does not depend on the detailed structure of the core potential, but only depends on the conduction electron density. Then, we have

singularity index we obtain the compact expression:

$$\alpha_b^{\text{TF}} = \frac{1}{2} \frac{1}{\pi a_0 k_F + 1}. \quad (11)$$

In the static ($\omega=0$) and small- k limits, ϵ_{TF} of Eq. (10) agrees with the more realistic dielectric function $\epsilon(\mathbf{k}, \omega)$ of Eq. (8). But for large k , $1/\epsilon_{\text{TF}}$ underestimates the screening effect. On the other hand, for large k , $\rho(\mathbf{k})$ of the point charge [$\rho(\mathbf{k})=1$] is overestimated compared with the more realistic one calculated from the Ashcroft pseudopotential [Eq. (4)]. Thus, some error cancellation between the underestimate of $1/\epsilon$ and the overestimate of $\rho(\mathbf{k})$ for large k takes place when we calculate Eqs. (9)–(11). The calculated values of α_b^{TF} of Na ($r_s=3.93$) and Al ($r_s=2.07$) are 0.198 (experimental value¹ of 0.20) and 0.128 (expt.¹ of 0.12), respectively. This good agreement with the experimental data is due to this error cancellation, although accidentally. However, it is rather effective over a wide range of electron density as shown by Fig. 3. We, thus, conclude that the present treatment, i.e., using the Thomas-Fermi dielectric function and a point charge for the core potential, is fairly good. According to Eq. (2), α must be less than 0.5 because of the Friedel sum rule. Equation (11) tends to 0.5 at the low electron density limit, which means that screening electrons are ascribed to only s wave electrons.

Figure 4 shows that the z_h dependence of the singularity indices, $\alpha^{\text{TF}}(z_h)$. Inside the metal $\alpha^{\text{TF}}(z_h)$ is enhanced near the metal surface just as shown in Fig. 1. As mentioned earlier, the first layer atom is located at a relatively large distance from the surface of electron gas. Hence, as with Fig. 1, we have the same conclusion about the surface singularity index; it is at most 5% larger than the bulk singularity index. Qualitatively speaking, the surface effect enhances the value of the singularity index but the surface effect is significant only when the atom is located within the characteristic screening length ($\lambda \sim k_{\text{TF}}^{-1}$) from the surface of electron gas. Actually,

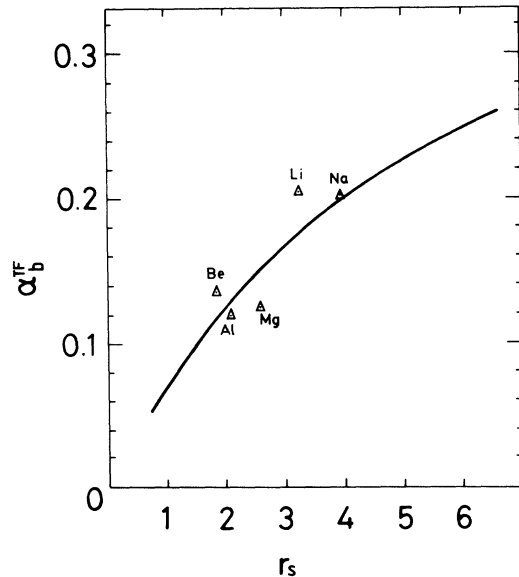


FIG. 3. The r_s dependence of the bulk singularity index, α_b^{TF} , calculated with the Thomas-Fermi dielectric function and the point-charge limit [Eq. (10)]. The triangles indicate the experimental data (Ref. 1).

however, the first layer atom is usually located deeper than λ from the surface of the electron gas. Therefore, the surface singularity index is almost the same as the bulk singularity index. This argument probably holds even for the case of the monovalent metals such as Au, Ag, and Cu.

In the vacuum ($z_h < 0$), the induced charge at the surface remotely screens the core-hole potential. Hence, $\alpha^{\text{TF}}(z_h)$ reduces its magnitude and approaches zero as the core-hole is away from the surface. $\alpha = 0$ means no asymmetry in the XPS line shape, i.e., the isolated atom limit.

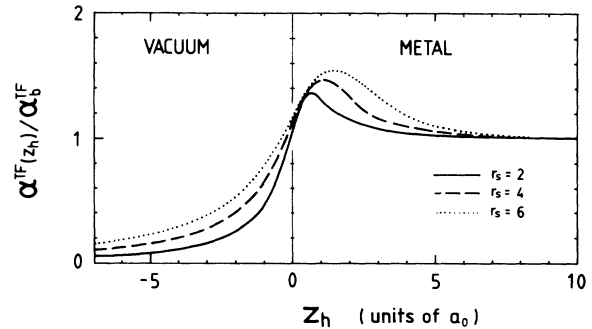


FIG. 4. The z_h dependence of the normalized singularity indices, $\alpha^{\text{TF}}(z_h)/\alpha_b^{\text{TF}}$, for three different electron densities. The calculation was carried out by Eqs. (9)–(11) (the Thomas-Fermi dielectric function and the point-charge limit).

Figure 4 is informative for estimating the singularity index of adsorbed atoms, particularly of physisorbed atoms such as Xe,¹⁶ where the bonding is due to weak van der Waal's force and has no significant charge transfer.

In conclusion, the DS line-shape function holds even at simple metal surfaces (Fig. 2), and the singularity index of the first layer atom is at most 5% larger than the bulk singularity index (Figs. 1 and 4). We expect the XPS from a physisorbed atom to show an asymmetric line shape in accordance with the z_h dependence with the z_h dependence shown by Fig. 4.

The author is much obliged to Dr. T. Chassé (Karl-Marx University, Leipzig) for his valuable suggestions and discussions. Part of this work was done when the author was at Waseda University. He also acknowledges clarifying discussions with Professor Y. H. Ohtsuki, Professor M. Kitagawa, and Dr. A. Ishii.

¹P. H. Citrin, G. K. Wertheim, and Y. Baer, *Phys. Rev. B* **16**, 4256 (1977).
²S. Doniach and M. Šunjić, *J. Phys. C* **3**, 285 (1969).
³D. M. Citrin, G. K. Wertheim, and Y. Baer, *Phys. Rev. B* **27**, 3160 (1983).
⁴P. Nozières and C. T. de Dominicis, *Phys. Rev.* **178**, 1097 (1969).
⁵G. Mahan, *Phys. Rev. B* **11**, 4814 (1975).
⁶P. Minnhagen, *Phys. Lett.* **56A**, 327 (1976).
⁷K. Shung and D. C. Langreth, *Phys. Rev. B* **28**, 4976 (1983).
⁸R. Brako and D. M. Newns, *J. Phys. C* **14**, 3065 (1981).

⁹D. C. Langreth, *Phys. Rev. B* **1**, 471 (1970).

¹⁰J. Chang and D. C. Langreth, *Phys. Rev. B* **8**, 4638 (1973).

¹¹D. M. Newns, *Phys. Rev. B* **1**, 3304 (1970).

¹²F. García-Moliner and F. Flores, *Introduction to the Theory of Solid Surfaces* (Cambridge University Press, Cambridge, England, 1979).

¹³J. Hubbard, *Proc. R. Soc. London, Ser. A* **243**, 336 (1957).

¹⁴N. D. Lang, *Solid State Commun.* **7**, 1047 (1969).

¹⁵G. K. Wertheim and L. R. Walker, *J. Phys. F* **6**, 2297 (1976).

¹⁶W. F. Egelhoff, Jr., *Surf. Sci. Rep.* **6**, 253 (1987), and references therein.